

Small-polaron transport in $\text{La}_{0.67}\text{Ca}_{0.33}\text{MnO}_3$ thin films

G. Jakob, W. Westerburg, F. Martin, and H. Adrian

Institut für Physik, Johannes Gutenberg-Universität Mainz, D-55099 Mainz, Germany

(Received 29 May 1998)

We present a detailed study of the activated resistivity of $\text{La}_{0.67}\text{Ca}_{0.33}\text{MnO}_3$ films up to 600 K under the influence of high magnetic fields. Data in zero field can be explained by small polaron hopping as treated in the Friedman-Holstein theory. Based on the spin orientation of ferromagnetic clusters in a magnetic field, we develop a phenomenological model describing the temperature and field dependence of the resistivity with a minimum of free parameters. We find that the polarons have a magnetic contribution to their activation energy for hopping which depends on the variation of the spin order with increasing temperature and can be modified by applied magnetic fields. The average magnetic clusters contain 4–6 ions. Hall measurements show a temperature dependent electronlike linear low field slope predicted by the theory of the Hall mobility of small polarons. [S0163-1829(98)04646-3]

I. INTRODUCTION

Since the discovery of colossal magnetoresistance effects in perovskitelike manganites a great interest has revived to investigate these doped ferromagnetic thin films. Published resistivity measurements in high magnetic fields on compounds such as $\text{La}_{0.67}\text{Ca}_{0.33}\text{MnO}_3$ (LCMO) concentrate on the temperature region from liquid helium temperature up to room temperature because of the wide availability of low-temperature magnet cryostats. Due to this limitation in temperature range and the relatively high Curie temperature T_C of these compounds systematic investigations of the resistivity in the paramagnetic regime over a broad temperature range under the influence of high magnetic fields are difficult to perform. As one solution Jaime *et al.*¹ used Gd doping in order to decrease the Curie temperature. In our study we renounce on additional doping but use specialized equipment to extend the temperature and field range.

Data of resistivity well above room temperature has only been reported in zero field,^{1,2} and it shows activated behavior given by

$$\rho(T) = \rho_0 T^\alpha \exp\left(\frac{E_A}{k_B T}\right) \quad (1)$$

with $\alpha=1$, according to the Emin-Holstein theory of adiabatic small polaron hopping.³ Other groups describe their data on similar compounds with variable range hopping^{4,5} or with the semiconductor formula containing a simple Boltzmann factor.⁶ Nevertheless the influence of high magnetic fields well above T_C on the activated resistivity has scarcely been investigated experimentally yet. Millis *et al.*⁷ and Sheng *et al.*⁸ solved in the mean field approximation microscopic models for the thermally activated transfer of charge carriers subjected to strong electron phonon coupling and polaron formation. Their solutions describe the qualitative behavior of the resistivity as function of temperature in a magnetic field. Motivated by this we developed a phenomenological model relating polaron transport to the mean field

magnetization of magnetic clusters in order to describe our measured temperature and field dependences of the resistivity quantitatively.

II. EXPERIMENT

Films were deposited on (100) MgO substrates by high-pressure on-axis dc-magnetron sputtering without further annealing. The chemical composition of the deposited films, as determined by Rutherford backscattering, was found to be identical to the nominal composition of the target ($\text{La}_{0.67}\text{Ca}_{0.33}\text{MnO}_3$). X-ray diffraction results showed a distorted cubic cell ($2a_0, 2a_0, 2a_0$) with $a_0=0.385$ nm and rocking angle analysis indicated epitaxial *a*-, *b*-, and *c*-axis oriented growth with an angular spread of 1° and 0.6° , respectively. The surface morphology of the samples was studied by scanning electron and by atomic force microscopy. An average grain size of 300 nm was found. The samples, typically 250 nm thick, were patterned photolithographically and etched to a 3 mm wide and 8 mm long bridge. The longitudinal resistivity was measured by the four-point technique. From liquid helium temperature up to room temperature we used a standard superconducting magnet cryostat. Above 300 K a different superconducting magnet system, which allowed room temperature access in fields up to 8 T, was required. We placed a small tube furnace with a 50 W heater into the room temperature bore in order to heat the sample up to 600 K. The cryostat wall was protected from warming by a vacuum insulation and a water cooled jacket. With this equipment, the whole temperature range between 4 and 600 K, in fields up to 8 T, could be investigated. The temperature-dependent measurements at constant field were performed in field steps of 1 T. Additionally we made field sweeps at several fixed temperature values. The procedure used for measurements of the Hall effect is described in detail elsewhere.⁹ A SQUID magnetometer was used to determine the magnetization.

III. RESULTS AND DISCUSSION

In Fig. 1 the temperature dependence of the resistivity in zero field and high magnetic fields is shown. For clarity only

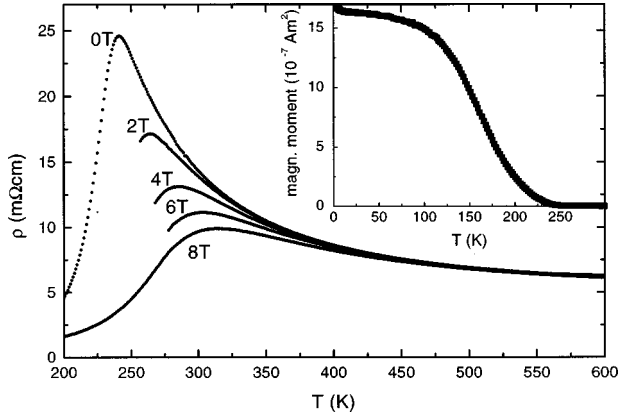


FIG. 1. Temperature dependence of the resistivity in zero field and in magnetic fields of $B = 2, 4, 6, 8$ T between 200 and 600 K. The curves for $B = 1, 3, 5, 7$ T are omitted for clarity. The inset shows magnetic moment vs temperature of the same sample at a field of $B = 20$ mT.

measured curves at even values of the magnetic field are plotted. The resistivity of the sample is metallic with a positive temperature coefficient at low temperatures. At higher temperatures the behavior changes to a thermally activated one. The temperature value of the resistance cusp is found by several authors to be close to the ferromagnetic ordering temperature T_C . For our sample the cusp is seen in zero field at $T_{\max}(B=0 \text{ T}) = 240$ K. Slightly below this temperature spontaneous magnetization is observed, as shown by the inset of Fig. 1. When a magnetic field is applied, the resistivity decreases. The cusp becomes less pronounced and shifts linearly to higher temperatures [$T_{\max}(B=8 \text{ T}) = 315$ K]. The curves are asymptotic to each other in the high-temperature regime. The analysis of the zero field curve according to Eq. (1) results in an exponent of the temperature-dependent prefactor of $\alpha = 1.6$. This indicates nonadiabatic small polaron hopping,¹⁰ which is identified by an exponent of 1.5. In the nonadiabatic approximation, there is only a small probability for the polaron to hop during the existence of the excited state where jumping is possible. In further calculations always the theoretical value of the exponent is used. In Fig. 2

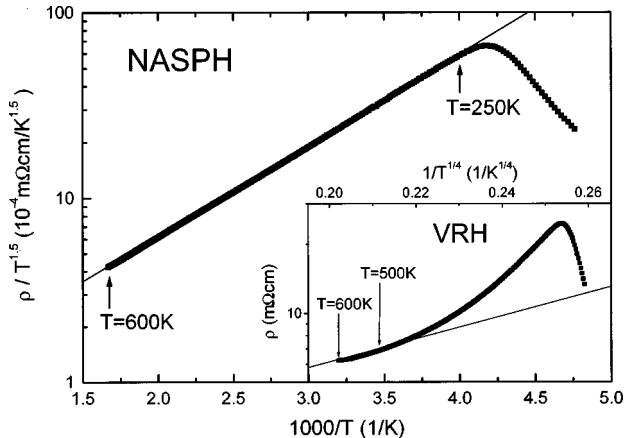


FIG. 2. The nonadiabatic small polaron hopping (NASPH) model explains the data over a temperature range of $\Delta T = 350$ K, while the variable range hopping (VRH) model in the inset does not fit the data.

we plot $\ln(\rho/T^{1.5})$ vs $1000/T$. An Arrhenius behavior, consistent with theory, is observed over a broad temperature range of $\Delta T = 350$ K. We have to mention here that in other samples we found an exponent nearly equal to 1, indicating polaron hopping in an adiabatic way.¹¹ However, a polaronic type of conduction yielded in all cases the best description. Other proposed models such as variable range hopping (VRH) and nearest-neighbor hopping are not able to fit our data, as can be seen easily for VRH from the inset of Fig. 2. The clear distinction between the different transport mechanisms is only possible due to the wide temperature range investigated in our experiment.

Equation (1) describes the motion of a polaron in an undistorted background trapped in its own potential. Here the localized carriers distort the surrounding lattice and magnetically polarize the manganese atoms in the neighborhood, thereby gaining exchange energy and forming a bound magnetic polaron. This concept was introduced by de Gennes.¹² Even well above T_C these magnetic polarons exist, as shown experimentally by de Teresa *et al.*¹³ with small-angle neutron scattering measurements and theoretically by Gehring and Coombes.¹⁴ In the case of the existence of magnetic polarons there is a magnetic exchange contribution to the activation energy. This form of phase segregation, finite ferromagnetic domains in a paramagnetic matrix, also explains measured magnetic susceptibility data.^{13,15} A phenomenological model taking into account a correlation between magnetization and resistivity was introduced by Núñez-Regueiro *et al.*⁶ He described the magnetization within a simple mean-field theory with the Brillouin function, but without regard to the formation of polarons. The field dependence of the activation energy in the case of manganites was additionally taken into account by Dionne.¹⁶ He expressed the activation energy by two terms. One is field independent and arises from electrostatic distortion, the other is field dependent and considers the exchange contribution. But also this model, which gives a linear dependence between the activation energy and the Brillouin function, is not able to fit our high-temperature data. The B^2 dependence of the magnetoresistance, shown by Snyder *et al.*,¹⁷ cannot be explained by this model, which gives only a linear dependence. Therefore we propose a phenomenological model with the following considerations.

The trapping of a ferromagnetic polaron is minimized by the transition of the paramagnetic neighborhood from random disorder to spin alignment due to an applied magnetic field. The main mechanism is the interaction between the spin of an unclustered single ion ($N_I = 1$) and the total spin of the ferromagnetic polaron containing a cluster of N_P ions. In the presence of a magnetic field the activation energy in Eq. (1) has to change to

$$E_A = E_A^0 (1 - \langle \cos \Theta_{IP} \rangle) \quad (2)$$

when only the spin is trapped. The nature of the polaron is almost purely magnetic and the electrostatic activation energy is only a minor correction.¹⁶ Here Θ_{IP} is the angle between the single ion spin and the cluster spin. If they are uncorrelated, it can be shown that $\langle \cos \Theta_{IP} \rangle = \langle \cos \Theta_I \rangle \langle \cos \Theta_P \rangle$. The average angle is related to the local magnetization by

TABLE I. Fitting parameters according to Eqs. (1) and (5) for three different samples. The values without (with) parenthesis correspond to the nonadiabatic (adiabatic) case.

Sample	A	B	C
ρ_0 (10^{-10} $\Omega\text{m}/\text{K}^\alpha$)	6.44 (209.7)	6.53 (211.4)	4.89 (157.2)
E_A^0 (meV)	120 (103)	96 (80)	133 (117)
T_C (K)	213.3 (203.6)	236.4 (235.9)	202.0 (195.6)
N_p	3.9 (5.9)	3.8 (5.0)	5.5 (7.8)

$$\langle \cos\Theta_{IP} \rangle = \frac{\langle M_I \rangle \langle M_P \rangle}{M_I^S M_P^S}. \quad (3)$$

In a mean field approximation the normalized magnetizations are expressed by the Brillouin functions $B_J(N_I=1, T - T_C, B)$ and $B_J(N_P, T - T_C, B)$:

$$\langle \cos\Theta_{IP} \rangle = B_J(N_I) B_J(N_P). \quad (4)$$

We used a g factor of 2 and with our nominal composition the average value of the angular momentum J is 2.28 (the manganese spins are 3/2 and 2). So the final modified Eq. (1) in magnetic field is

$$\rho(T, B) = \rho_0 T^\alpha \exp\left(\frac{E_A^0}{k_B T} [1 - B_J(N_I) B_J(N_P)]\right). \quad (5)$$

By using Eq. (1) and $\alpha = 1.5$ the zero field resistivity curve was fitted. Thus the fitting parameters ρ_0 and E_A^0 , listed in Table I, were fixed. A fit of the measured temperature dependence for one fixed value of the magnetic field using Eq. (5) allowed us to determine the two other fitting parameters N_p and T_C . All other field curves can be described now by Eq. (5) without further free parameters, with the field and temperature dependence given by the Brillouin function. The result of the analysis is shown by lines in Fig. 3(b). The correspondence between the experimental data (points) and the fitting values is surprisingly good. T_C is 233 K, which corresponds with the onset of the magnetization, as can be seen by the inset of Fig. 1. The cluster size N_p is 3.8 ± 2 , i.e., only the nearest neighborhood is spin polarized. The uncertainty of the cluster size can be seen by inspection of Fig. 3(a) and 3(c). They show the best possible fits when the cluster sizes are fixed, with values $N_p = 1$ and $N_p = 7$, respectively. The first value represents a model of pure electron hopping that takes into account spin-dependent barrier energies. There is an obvious disagreement between experiment and the fit for these choices of the cluster sizes. The numerical value for N_p should not be considered as exact, however, it demonstrates that a small finite cluster size is necessary to describe the experimental data. The zero-field fit curve exhibits no maximum, because fluctuation effects are not taken into account and therefore the calculated magnetization is exactly zero above T_C . For applied magnetic fields the model describes the linear shift and the height of the cusp in the resistivity, in the range from 250 K and 1 T to 315 K and 8 T, with only one value of T_C . With the same parameters used in Fig. 3(b) also $\rho(B)$ is reproduced, as is demonstrated in Fig. 4. Our model describes the B^2 dependence of the magnetoresistance resulting from the field dependence

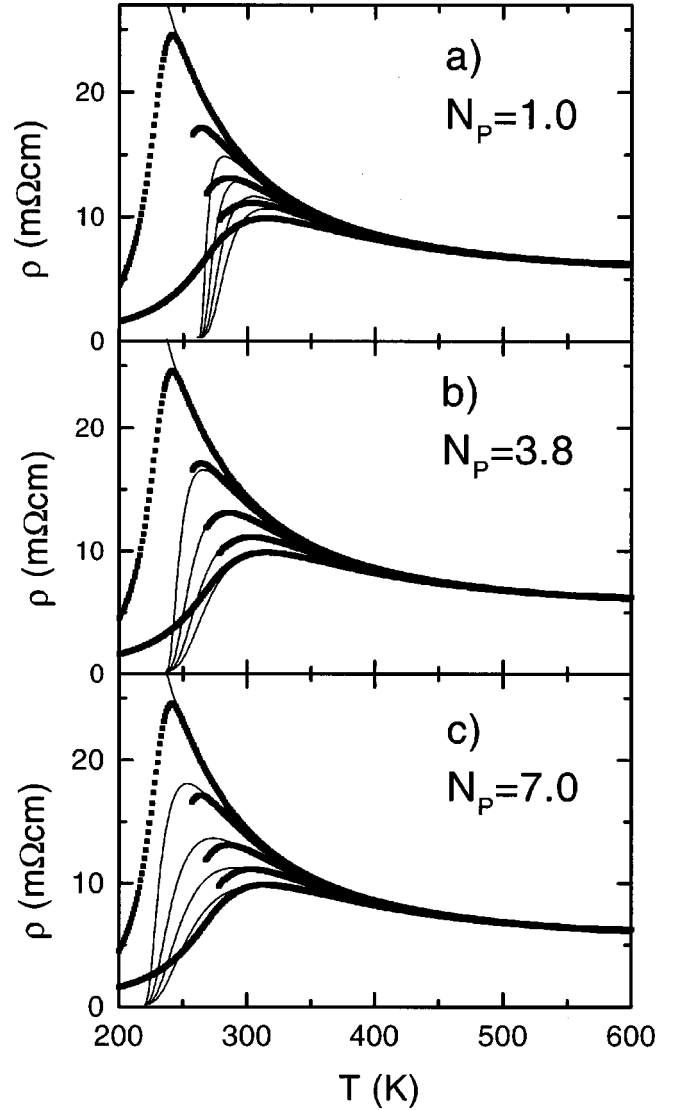


FIG. 3. Experimental data and fitting curves for various cluster sizes according to Eq. (5).

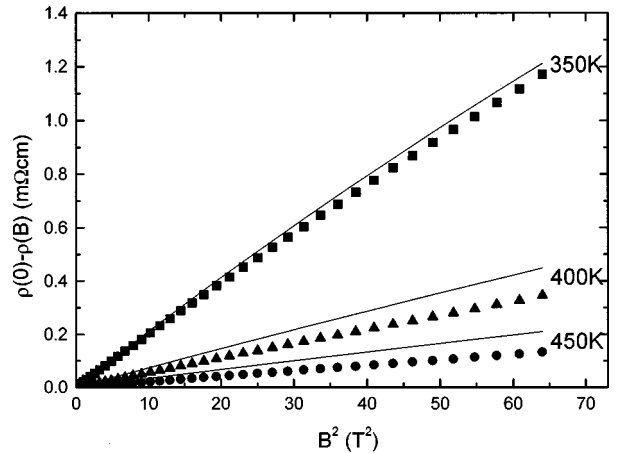


FIG. 4. Measured resistivity as a function of magnetic field for constant temperatures (symbols). The straight lines are calculated from Eq. (5) using the same parameters as in Fig. 3. The B^2 dependence of the magnetoresistance resulting from the field dependence of the activation energy is seen for the measured curves.

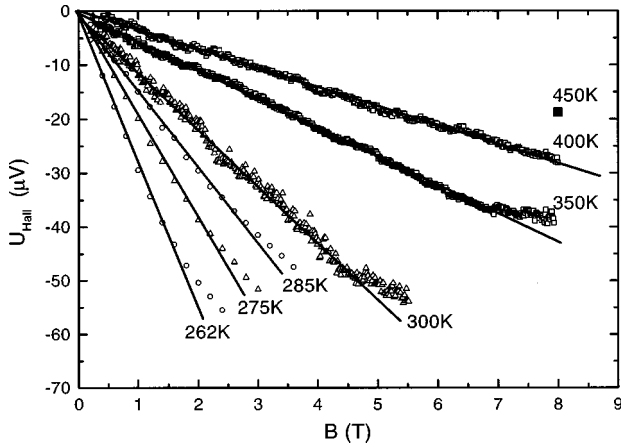


FIG. 5. Measured Hall voltages as a function of magnetic field for constant temperatures. The straight lines represent a linear fit of the low field values.

of the activation energy above T_C . This is only possible, if the activation energy is decreasing quadratically with the Brillouin function. Three samples were measured and the corresponding fitting parameters are listed in Table I. The values with and without parenthesis correspond to the adiabatic ($\alpha=1$) and nonadiabatic ($\alpha=1.5$) case, respectively. In both regimes a finite, small cluster size was found for all samples.

Further evidence of polarons in the manganites results from Hall effect measurements. Friedman and Holstein¹⁰ found that for motion between three equivalent sites the Hall effect is electronlike for both electron and hole conduction. The Hall current is a quantum interference effect. The interference between the probability amplitude for direct jumps and for jumps involving virtual occupation of a third site results in a change of the jump rate which is linear in B . This electronlike linear slope of the Hall voltage in the paramagnetic regime for different temperatures is plotted in Fig. 5. The straight lines correspond to a linear fit. The linear dependence is only valid for low fields and high temperatures, because with applied magnetic field or by cooling a phase transition from localized to delocalized states is induced and the theory of polarons is no longer valid. These considerations are published elsewhere.⁹ The theory also predicts a temperature dependence of the Hall coefficient of $R_H \propto T \exp(2E_A/3k_B T)$, which is similar to the temperature dependence of the longitudinal resistivity in the adiabatic limit, but with a lower Hall activation energy. This was experimentally found by Jaime *et al.*¹ The Hall coefficients calculated from the slopes of the Hall voltage yield a straight line in the Arrhenius plot in Fig. 6. The activation energy of the Hall mobility (160 meV) for sample B is in our experiment higher than the activation energy of the drift mobility (96 meV).

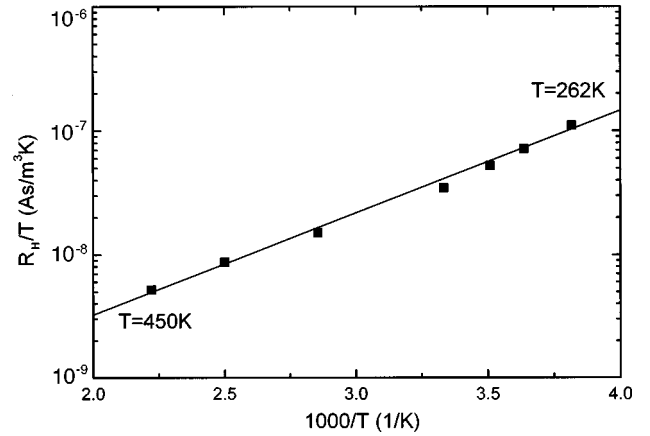


FIG. 6. Temperature dependence of the electronlike low field slope.

This is in contradiction with the theory of Friedman and Holstein developed for a triangular lattice. However, a more general theory of Schnakenberg¹⁸ found the same activation energy for both jump processes.

IV. CONCLUSION

We performed detailed high field transport measurements of the colossal magnetoresistive compound $\text{La}_{0.67}\text{Ca}_{0.33}\text{MnO}_3$. Our temperature range covered the paramagnetic regime from the ferromagnetic ordering temperature near room temperature up to 600 K ($2.5 T_C$). This wide range above room temperature enabled us to distinguish different transport mechanisms without additional doping. We demonstrated that the high-temperature resistivity data of thin manganite films can be explained by small polaron hopping. The field dependence requires the concept of a magnetic polaron. We proposed a phenomenological model describing quantitatively the temperature and field dependence of the resistivity. It reproduces the resistivity cusp and the B^2 dependence of the magnetoresistance. For best fits we found small clusters containing 4–6 ions, i.e., only nearest neighbors are spin polarized. The activation energy for the polaronic Hall effect was found in our work to be higher than that for longitudinal transport.

ACKNOWLEDGMENTS

We thank P. Gütlich from Institut für Anorganische Chemie und Analytische Chemie for usage of the magnet cryostat with room temperature access and J. Geerk from Forschungszentrum Karlsruhe for the Rutherford backscattering analysis of the film stoichiometry. This work was supported by the Deutsche Forschungsgemeinschaft through Project No. JA821/1.

¹M. Jaime, H. T. Hardner, M. B. Salamon, M. Rubinstein, P. Dorsey, and D. Emin, Phys. Rev. Lett. **78**, 951 (1997).

²D. C. Worledge, G. J. Snyder, M. R. Beasley, T. H. Geballe, R. Hiskes, and S. DiCarolis, J. Appl. Phys. **80**, 1 (1996).

³D. Emin and T. Holstein, Ann. Phys. (N.Y.) **53**, 439 (1969).

⁴P. Wagner, V. Metlushko, L. Trappeniers, A. Vantomme, J. Vanacken, G. Kido, V. V. Moshchalkov, and Y. Bruynseraede, Phys. Rev. B **55**, 3699 (1997).

⁵M. Viret, L. Ranno, and J. M. D. Coey, Phys. Rev. B **55**, 8067 (1997).

- ⁶J. E. Núñez-Regueiro and A. M. Kadin, *Appl. Phys. Lett.* **68**, 2747 (1996).
- ⁷A. J. Millis, B. I. Shraiman, and R. Mueller, *Phys. Rev. Lett.* **77**, 175 (1996).
- ⁸L. Sheng, D. Y. Xing, D. N. Sheng, and C. S. Ting, *Phys. Rev. Lett.* **79**, 1710 (1997).
- ⁹G. Jakob, F. Martin, W. Westerburg, and H. Adrian, *Phys. Rev. B* **57**, 10 252 (1998).
- ¹⁰L. Friedman and T. Holstein, *Ann. Phys. (N.Y.)* **21**, 494 (1963).
- ¹¹G. Jakob, F. Martin, W. Westerburg, and H. Adrian, *J. Magn. Mater.* **177-181**, 1247 (1998).
- ¹²P. G. de Gennes, *Phys. Rev.* **118**, 141 (1960).
- ¹³J. M. De Teresa, M. R. Ibarra, P. A. Algarabel, C. Ritter, C. Marquina, J. Blasco, J. Garcia, A. del Moral, and Z. Arnold, *Nature (London)* **386**, 256 (1997).
- ¹⁴G. A. Gehring and D. J. Coombes, *J. Magn. Mater.* **177-181**, 873 (1998).
- ¹⁵J. Z. Sun, L. Krusin-Elbaum, A. Gupta, Gang Xiao, and S. S. P. Parkin, *Appl. Phys. Lett.* **69**, 1002 (1996).
- ¹⁶G. F. Dionne, *J. Appl. Phys.* **79**, 5172 (1996).
- ¹⁷G. J. Snyder, M. R. Beasley, T. H. Geballe, R. Hiskes, and S. DiCarolis, *Appl. Phys. Lett.* **69**, 4254 (1996).
- ¹⁸J. Schnakenberg, *Z. Phys.* **185**, 123 (1965).